AutoSense: Unobtrusively Wearable Sensor Suite for Inferring the Onset, Causality, and Consequences of Stress in the Field*

Emre Ertin
The Ohio State University
Columbus, OH 43210

ertin.1@osu.edu

Nathan Stohs
The Ohio State University
Columbus, OH 43210

stohs.3@osu.edu

Santosh Kumar
University of Memphis
Memphis, TN 38152

skumar4@memphis.edu

Andrew Raij
Universit of South Florida
Tampa, FL 33620

raij@usf.edu

Mustafa al'Absi
University of Minnesota
Duluth, MN 55812

malabsi@umn.edu

Siddharth Shah
The Ohio State University
Columbus, OH 43210

shah.561@osu.edu

Abstract

The effect of psychosocial stress on health has been a central focus area of public health research. However, progress has been limited due a to lack of wearable sensors that can provide robust measures of stress in the field. In this paper, we present a wireless sensor suite called AutoSense that collects and processes cardiovascular, respiratory, and thermoregularity measurements that can inform about the general stress state of test subjects in their natural environment. AutoSense overcomes several challenges in the design of wearable sensor systems for use in the field. First, it is unobtrusively wearable because it integrates six sensors in a small form factor. Second, it demonstrates a low power design; with a lifetime exceeding ten days while continuously sampling and transmitting sensor measurements. Third, sensor measurements are robust to several sources of errors and confounds inherent in field usage. Fourth, it integrates an ANT radio for low power and integrated quality of service guarantees, even in crowded environments. The AutoSense suite is complemented with a software framework on a smart phone that processes sensor measurements received from AutoSense to infer stress and other rich human behaviors. AutoSense was used in a 20+ subject real-life scientific study on stress in both the lab and field, which resulted in the first model of stress that provides 90% accuracy.

Categories and Subject Descriptors

C.5.3 [**Computer System Implementation**]: Portable Devices; J.4 [**Computer Applications**]: Social and Behavioral Sciences

General Terms

Design, Experimentation, Measurement, Human Factors

Keywords

Wearable Physiological Sensors; Psychological Stress Monitoring; Mobile Health; Deployment Experiences

1 Introduction

Repeated exposures to stress can cause physical illnesses (e.g., headaches, fatigue, difficulty sleeping, and heart diseases), behavioral issues (e.g., addiction, attention deficit, and depression), and social issues (e.g., loneliness, anger, and setbacks in personal and professional relationships) [27]. Novel mobile applications can be developed for stress management, if stress can be reliably monitored in real-life. Robust inferencing of stress in the natural environment, however, has proven extremely challenging due to a lack of unobtrusively wearable devices that can provide scientifically valid measurements of various physiological responses to stress, from uncontrolled natural environments, as demanded in health applications [33].

In this paper, we present *AutoSense*, an unobtrusively wearable wireless sensor suite that can collect continuous measurements for inferencing of stress, its causes, and consequences, in the natural environment of individuals. The selection of sensors, hardware design and algorithms for managing energy consumption is designed and optimized from the ground up with the stress inference application in mind. AutoSense focuses on physiological measures monitoring cardiovascular, respiratory, and thermoregulatory systems, since these systems are modulated by both psychologically and physically demanding conditions. AutoSense combines six sensors into a conveniently wearable chest band — two lead Electrocardiogram (ECG) measurement of electrical activity of the heart; respiratory inductive plethysmograph (RIP) band for measurement of relative lung volume and breathing rate at the rib cage; galvanic skin response (GSR) between the two ECG electrodes; skin temperature thermistor under the arm; an ambient temperature sensor, and a three-axis accelerometer to assess motion artifacts in the data and provide inferences about the subjects' physical activities. The sensors selected in AutoSense are those that

have been found to be most discriminating [8, 12, 13, 26] for detecting stress and affect, yet are unobtrusively wearable.

AutoSense integrates all six sensors, bioamplifiers, and TI MSP430 and nRF24AP2 transceiver from Nordic semiconductor onto a 1x2.5 square-inch circuit board. This includes a 750 mAh battery with built in USB charging and battery monitoring circuits. We also designed a Bluetooth to ANT (nRF24AP2) bridge to wirelessly communicate with a smart phone. Figure 1 shows a picture of the AutoSense sensor suite and the bridge in its custom plastic packaging. All sensor boards include digital sensor/radio power switches for duty cycling of the sensors and radio in software.
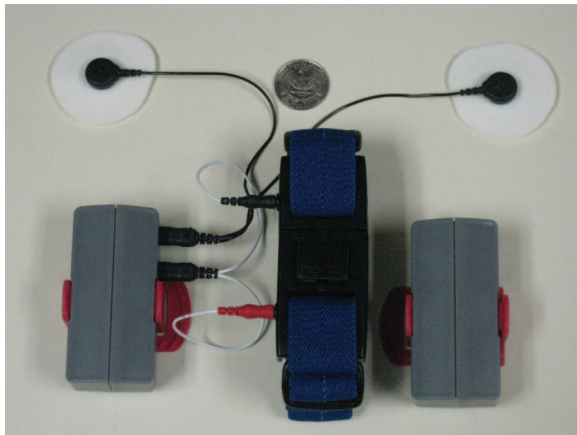

Figure 1. The AutoSense sensor suite in its packaging. ECG leads and RIP connectors plug in to the unit on the side. When worn, the red clip is used to attach the unit to the (blue) RIP band that goes around the chest. The Bluetooth to ANT (nRF24AP2) bridge is also shown.

For ease of wearability, the ECG and GSR share a common electrode. For unobtrusive wearing, the GSR is placed at the chest rather than its usual placement on fingers or earlobes. For added protection to subjects with health conditions, high impedance circuitry is used to limit current flow, even in the case of external events (e.g., through physical breaking of the sensor board or shorting of the battery leads). For robust respiration measurement in the field, inductive plethysmography is used instead of a piezoelectric band [7].

AutoSense incorporates several innovations in the design of sampling and wireless communication. It integrates ANT (nRF24AP2) radio for low power and quality of service guarantee with built-in TDMA. We evaluated the loss in antenna performance due to proximity to human body, and found a 33% loss of power if the traditional design is used, which is optimized for free space placement. We determine the best matching gain to reduce the loss of power to 0.1%. Next, we determined the frequency range of ANT that is immune to interference from Wi-Fi (they share the same ISM band). We also developed appropriate buffer management so that measurements from all six sensors are sampled at the appropriate frequency and communicated on a single radio, all managed by a single microcontroller. The short packet structure of ANT required minimizing header overhead. This required innovation in the structure of the header so losses in

the wireless channel can be identified and associated with the appropriate sensor type at the receiver.

AutoSense is complemented with a software framework on the mobile phone, called *FieldStream*, that receives measurements from AutoSense, computes a variety of features from the measurements, and makes behavioral inferences. These inferences include stress level and other behaviors related to stress (e.g., activity and conversation).

AutoSense and FieldStream platforms have been used in a real-life behavioral science lab and field study on 21 human subjects. The subjects underwent four stress sessions in the lab and wore AutoSense for 2 full days in field. Measurements obtained from AutoSense enabled the development of new stress models that provide high accuracy in both lab and field settings [23]. A survey conducted at the end of the study shows that participants found AutoSense comfortable to wear for long hours in the field. AutoSense has also been used by 30+ subjects in another study where they wore it for 3 days in the field. It is currently being used by 50+ subjects for scientific studies of stress and addictive behavior where each subject is wearing it for 1-4 weeks in the field.

Organization. In Section 2, we explain our rationale for picking the set of sensors for AutoSense. Section 3 describes the hardware design of sensors, while Section 4 describes the design of the sampling and communication subsystems. Section 5 describes the FieldStream software framework, Section 6 describes real-life deployment experience, and Section 7 discusses some related works. We conclude the paper in Section 8 and discuss some future work.

2 Selecting the Set of Sensors for AutoSense

The term *stress* refers to a broad range of psychological processes, and, therefore, it is exceedingly difficult to come up with a single physiological measure that can be used as a universal marker across distinct stress conditions. The aim of AutoSense is to monitor psychosocial stress in the daily life of subjects, in an unobtrusive way, over an extended period of time. In previous works [8, 12, 13, 26], physiological measures of heart-respiration rate and its variability, blood pressure, eye activity, skin conductivity, muscle activity, and skin temperature have been found to respond to stress.

The biological approach to monitoring stress focuses on activation of physiological systems which are known to react to physical and psychological demands. The two primary systems of stress indicators are the Hypothalamic-pituitary-adrenocortical axis (HPA) and the Sympathetic-adrenal medullary system (SAM). The HPA axis deals with hormonal responses to excessive stimulation of the adrenal cortex, which results in secretion of cortisol hormone. This is part of of the human adaptive mechanism for maintaining function under changing environmental conditions. Since HPA axis plays a central role in the body's psychobiological stress response, cortisol measurements are used heavily in stress research. While ambulatory methods of cortisol measurement exists in the form of saliva, blood, or urine sampling at regular intervals, they are not suitable for continuous monitoring of stress [21] due to subject burden.

SAM, on the other hand, deals with the autonomic nervous system (ANS) response to changing environmental de-

mands. The ANS consists of two subsystems — the sympathetic system (SS), associated with energy mobilization, and the parasympathetic system (PS), associated with vegetative and restorative functions. These two subsystems (acting like gas and break pedals in a car), keep the cardiac functions in dynamic balance. In particular, heart rate is under the control of the ANS such that relative increases in sympathetic activity leads to increases in the heart rate and relative increases in parasympathetic activity are associated with decreases in heart rate [30]. Therefore, the analysis of time intervals between heartbeats, referred as heart rate variability (HRV) analysis, provides information on relative activation of SS and PS. Typically, HRV analysis relies on frequency domain analysis of the interbeat time interval series due to the known time constants of SS and PS. Sympathetic system regulation can only occur at slow time scales and therefore its effect on HRV rolls-off at 0.15 Hz, whereas parasympathetic influences can occur at faster time scales up to 0.4 Hz. Therefore, high-frequency HRV (0.15-0.4 Hz) represents pure parasympathetic influences whereas low frequency HRV (0.04-0.15 Hz) has a mixture of sympathetic and parasympathetic influences. Monitoring HRV energy in these two bands can inform on SS/PS balance and consequently about body's stress response. HRV analysis requires interbeat time intervals. Thus,, commonly used heart rate monitors which average heart rate over tens of seconds are not sufficient. AutoSense employs digital filtered ECG waveforms for accurate analysis of HRV. However, the ECG sensor by itself is not suitable for conducting stress studies that examine ANS cardiac control across subjects. This is mainly because HF-HRV is also affected by respiration rate, tidal volume (displaced air during respiration) and posture (supine/standing). To control for these effects, AutoSense includes a respiration band to measure respiration rate and tidal volume as well as a 3-axis accelerometer for detection of body orientation and activity. In addition, the respiration band and accelerometer is used for detecting speech and intensive physical activity episodes where the link between HRV and stress response is harder to assess.

Finally, AutoSense includes skin conductance, body and ambient temperature to monitor activation of thermoregulatory and nervous systems of the body. Although the primary function of endocrine sweat glands is cooling, those located on the palmar and planter surfaces are involved in grasping behavior. As a result, these surfaces are more responsive to emotional stimuli, associated with the "fight or flight" reflex [2]. These sensors provide information that can be used in monitoring the flight-or-fight response of the nervous system, after factoring the effects of body heat flow. In summary, AutoSense provides a carefully designed sensor suite for precise measurement and analysis of ANS stress response that can be worn unobtrusively in the natural environment for long periods of time.

3 AutoSense Sensor System — Hardware Design

In this section, we describe the hardware design of the AutoSense sensor suite and its evaluation against commercially available units. AutoSense embodies the following six sensors onto a mote (i.e., TI MSP430) hardware — *Two Lead electrocardiogram (ECG)* for measurement of electricity of the heart, *Respiratory inductance plethysmography (RIP) sensor* integrated into a chest band for relative lung volume and breathing rate at rib cage, *Galvanic skin response (GSR)* under the band via the ECG electrodes, *Skin temperature sensor* placed under the band for monitoring the thermoregulatory response to stress, *Ambient temperature sensor* embedded into the mote hardware for heat flow calculations in tandem with the skin temperature sensor, and *3-axis accelerometer* for motion sensing, used to assess motion artifacts of the data and provide general activity and rest information for the subjects. The sampling frequencies of these sensors are described in Section 4.5.1. The sensor node processes ECG and respiration band signals to extract beat-to-beat heartrate information and to filter out noise. This enables a continuous detailed study of heart rate variability (or more precisely variability of individual cardiac periods) to assess changes in autonomic control of cardiac functions.

3.1 Respiratory Sensing

Respiration rate has been linked to various stressors in laboratory studies. However, there is no direct non-invasive way of measuring respiration rate. The most accurate measurement of respiratory effort is through esophageal manometry. In this method, a catheter is inserted in the esophagus to measure air pressure directly. A nasal thermistor can inform about the respiration rate but not the respiration effort. Impedance plethysmography methods pass a weak alternating electric current through two or more electrodes and measure impedance. Changes in this impedance can be linked to thoracic and abdominal movement during breathing. The frequency range of the alternating current source have to be chosen carefully not to interfere with pacemakers, defibrillators and other sensors, such as ECG and GSR. These methods are obtrusive and not suitable for field studies where the subjects have to continue with their daily routine. Our approach to respiratory sensing uses an elastic band to measure relative lung volume through sensing changes in the tension as the chest expands or contracts. This surrogate measure to respiratory effort is known as plethysmography. We evaluated two alternative approaches for plethysmography — piezoelectric sensors and inductance-based sensors.

Piezoelectric sensors are the most common method in use and rely on a piezoelectric crystal placed where the two ends of the band connect. The crystal generates a voltage when compressed or stretched, correlated with chest wall displacement. While inexpensive and simple to integrate into a mote based system, in our experiments, we found the piezo-based method was prone to the so-called "trapping" artifact. While the subject engages activities in their daily life, often the particular portion of the band where the sensor is placed can become trapped which can significantly under or overestimate the tension along the circumference. The artifact is most troublesome when the person is laying down or leaning against furniture. In addition, often a change in body position leads to a different steady state load on the piezo sensor, causing sudden jumps in respiratory readings.

Respiratory inductance plethysmography (RIP) uses a conductive thread that is sewn in a zigzag fashion to the elas-

tic band. An alternating current source is applied to the resulting loop of wire, which, in turn, generates a magnetic field that opposes the current whose strength is proportional to the area enclosed by the wire (according to Lenz's law). The ratio of the magnetic flux to the current is called self-inductance. Therefore, changes to the chest circumference can be measured by measuring the changes to the self inductance of the band. The inductance measurement depends purely on the geometry of the band and is not related to the tension in the band. As a result, the measurement is not prone to the trapping of the band and associated artifacts due to changes in tension. There are many commercially available bands with embedded wire threads. These bands are often sold with propriety electronic boards that measure the inductance and produce a voltage that makes them compatible with recorders intended to be used with piezoelectric sensors. These conversion boards are not suitable for integration with the AutoSense system due to their size, power consumption, and cost.

We designed a new sensor board for RIP bands for low power sensing and direct integration with the mote hardware. The band is used in series with a known inductor to set the frequency of a Colpitt's oscillator (nominally 400 kHz in our circuit). Then, the output of the oscillator is shifted by adding a DC bias and fed to a zero-crossing counter. The zero crossing counter output is integrated and low-pass filtered before an instrumentation amplifier that amplifies and subtracts the long term baseline before the Analog-to-Digital sampling. Figure 2 shows the respiratory signal obtained through the RIP sensor, with features of respiration marked. Although the morphology of the respiratory effort signal is less well known than for ECG, several studies have shown the potentially rich information contained in the respiratory effort signal. Various features obtained from respiration (see Figure 2) have been shown to be good markers of speaking [18], stress [8], and emotion [12, 13, 26]. These works, however, were conducted in supervised laboratory conditions, since a RIP sensor that can provide good quality measurements in the field was unavailable. Development of our RIP sensor enables collection of respiration measurements in the natural environment and inferring the conversation status of a subject in real-time on a mobile phone with $> 87\%$ accuracy [24].
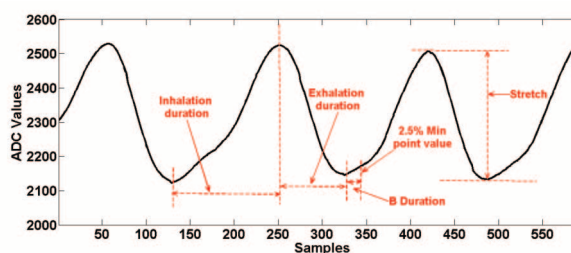

Figure 2. Features computed over respiration measurements that are used in detecting stress and conversation.

3.2   Integrated ECG and GSR Sensing

Electrocardiography (ECG) sensing is the primary method for assessing cardiovascular activity in subjects. The sinoatrial node produces electrical impulses to stimulate heart muscles and control the pumping action of the heart. ECG measures this electrical activity through electrodes applied to the skin. In particular, electrodes placed on different sides of the heart measure activity at different parts of the heart. A two lead ECG informs about the overall rhythm of the heart, providing precise timing information of the heart beat intervals. A multiple lead ECG sensor measures potentials across different vectors across the heart and can indicate problems or weakness in particular parts of the heart muscle.

In AutoSense, we are interested in the timing of the heart beats and, therefore, use the standard two-lead configuration measuring potential from left to right. The typical potential across the heart is a small magnitude on the order of 1mV which must be amplified by a factor of 100 before the sampling circuit. The electric field interference from power lines and other electrical equipment can cause signals of similar magnitude unless differential amplifiers with high common-mode rejection is employed. A second problem with two-lead systems is baseline wander since the third grounding leg electrode is missing. In addition, electrode-skin impedances can vary between the two electrodes, leading to source a impedance unbalance, which produces differential mode voltage that will be amplified by the differential amplifier. Therefore, the baseline needs to be extracted and abstracted from the main signal to provide the maximum dynamic range of the ADC. As discussed next, this baseline correction circuit provides a way to integrate galvanic skin response sensing into the same electrode through applying a fixed, known differential between the electrodes. Finally, appropriate analog filtering must be employed to attenuate high frequency noise sources and to prevent aliasing in the analog-to-digital sampling stage.

Galvanic Skin Response (GSR) measurements are conducted by applying a known DC or AC potential across two electrodes and measuring resistance across the terminals. Simple bridge circuits are used to measure variations from a nominal resistor value. This simple sensor usually requires an extra set of electrodes that are placed with the sensor. To maximize comfort and simplify the procedure for wearing the band, we integrated ECG and GSR sensors onto the same electrode. In addition to reducing the required number of electrodes, GSR readings, in turn, provide valuable information that is used in ECG signal processing, since they inform about the long term signal levels. A differential voltage bias is applied to the two electrodes through a bridge circuit. The GSR circuit measures the potential on the electrodes using a single stage differential amplifier. The ECG circuit uses a high impedance amplifier to measure the variation across the electrodes without loading the circuit. A second instrumentation amplifier with baseline correction amplifies the signal by 5. After baseline correction and centering, a final amplifier applies a gain of 100 and performs low pass filtering with a cutoff of 60 Hz.

3.3 Temperature and Accelerometer Sensors

The AutoSense system measures relevant simple skin responses. The skin conductance is directly proportional to skin moisture content correlated with stress in many studies [8, 12]. The skin temperature gradient has been also been suggested as an indicator of stress [14] and also indicates the environmental conditions for the subject. AutoSense motes have two temperature sensors to measure body and ambient temperature. For body temperature, a medical-grade glass-bead thermistor is used with a simple bridge circuit to measure body surface temperature. For the ambient temperature, we use a low power analog temperature sensor for measuring ambient temperature on the mote surface. We use the ADXL335 three-axis accelerometer from Analog devices with simple RC low pass filters on each channel to measure acceleration using independent ADC channels.

3.4 Comparison of the ECG and RIP sensor measurements with Commercial Sensors

To compare the ECG and RIP sensors of AutoSense with commercially available sensors (which are intended for use in controlled settings), we collected data simultaneously with commercially available sensors across various activity profiles (sitting, walking, running) on a treadmill. For ECG, we used the Garmin Forerunner 305, a GPS enabled watch that monitors heart rate via a wireless chest strap. The watch was worn around the wrist of the subject, while the chest strap was fitted around the subject's chest at the height of the sternum. The AutoSense sensor suite was attached to the RIP band that the subject wore slightly above the Garmin strap. The data was then transmitted via a Bluetooth bridge to a phone kept with the subject throughout the test. The phone stored this data for later analysis. We collected heart rate data over 200 minutes over multiple sessions. Figure 3 shows measurements from both of these ECG sensors for a typical session.

For the respiration, we used the commercially available RIP sensor from Sleepsense and a similar experimental set up as for ECG. Sleepsense's inductive effort sensor requires an external ADC unit and is geared towards sleep research. The output of the Sleepsense sensor utilizes a heavier low pass filtering circuit to provide signals suitable for sleep researchers. To maximize correlation to the Sleepsense signals, we low-pass filtered AutoSense RIP output with a digital 4 Hz filter and calculated a linear fit model for the raw respiration signals provided by the two sensors. For each activity profile, we evaluated goodness of fit using the R^2 coefficient. As shown in Table 1, we get a good correlation with the commercial sensors for various activity profiles, validating the measurements obtained from AutoSense sensors.

4 Sampling and Wireless Communication

The main function of the AutoSense sensors is to sample and transmit physiological data streams to the user's mobile phone. The physiological signals are sampled at sampling frequencies that are determined by the frequency content of each signal, resulting in fixed rate downlink traffic. It is well known that for low-power radios utilized in sensor node design, operating the receiver and the transmitter sections consume approximately the same power. Conse-
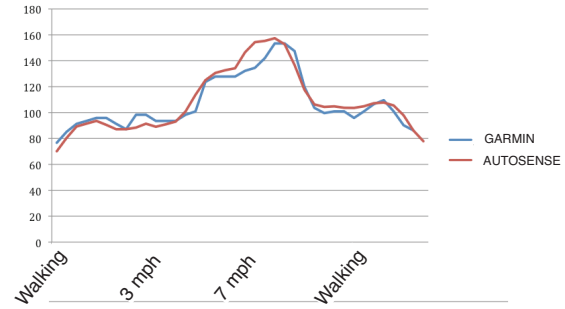

Figure 3. Example Validation Session for Heart Rate

Activity	Garmin-AutoSense Heart Rate	Sleepsense-AutoSense RIP signal
Sitting	0.93	0.89
Walking	0.90	0.86
Run (3.0 mph)	0.91	0.82
Run (5.0 mph)	0.86	0.79

Table 1. Goodness of Fit (using the R^2 coefficient) for AutoSense and Garmin/SleepSense Signals

quently, power cycling the receiver is a widely adopted strategy for reducing radio power consumption. For fixed rate traffic, Time Division Multiple Access (TDMA) provides a means to power-cycle *both* the receiver and the transmitter in a network. TDMA also helps maintain the data rate and transmission schedule of existing sensors when additional sensors are added on to the body, since they can be allocated different time slots. Moreover, in user studies, several subjects (who may be students at a university) may spend significant time in close vicinity of each other (such as when taking a class together). TDMA is able to scale with minimal overhead per packet in such crowding situations by providing separation along channels and time slots.

Radio Selection. Although software solutions for TDMA can be implemented with 802.15.4 radios, we selected the Nordic Semiconductor nRF24AP8 transceiver chip for sensor data transmissions and back-channel control messages. Nordic Semiconductor nRF24AP8 is a bidirectional radio transceiver with built in firmware implementing the ANT protocol developed by Dynastream Innovations Inc. nRF24AP8 operates in the 2.4 GHz ISM band. The ANT protocol provides a TDMA based Channel Access scheme with an optional network layer supporting point-to-point, star, tree, and mesh network topologies [1]. The raw data rate of the radio is 1 Mbit/s. The packet payload size is optimized for slow data rate sensors at short packets of 8 bytes/packet. Neighbor discovery, channel allocation, and the TDMA protocol is handled by the transceiver chip, allowing coexistence with other ANT enabled sensors. Currently, the ANT platform is primarily adapted for low-rate devices such as heart rate monitors, wrist watches, and bicycle computers. AutoSense provides a data stream that is at a higher rate than

most existing devices adopting ANT technology, with an approximate data rate of 1.8 kbits/s.

Bluetooth to ANT Bridge. ANT radios are available on very few smart phones; even fewer expose it to developers. Until they become widely available, additional effort is needed to facilitate wireless communication between ANT sensors and smart phones. One could use nRF24AP8-based dongles that plug in to a phone's USB port. But, this increases the form factor of the phone. Alternatively, Bluetooth radio can be integrated onto a sensor node itself [15], but Bluetooth radio can drain the battery that is shared with the sensors. Low-power bluetooth, when available widely, can help address this issue.

To accommodate a wide variety of smart phones available today, we have added a bridge node in between the wearable sensors and the mobile device as in [6]. A bridge node can help pair up any mobile phone with any ANT sensor without introducing strong coupling requirements.

In our design, we connect the BlueTooth serial module (BlueRadio-CR46AR) to the UART1 lines of the MSP430. We minimize packet loss using a queueing mechanism on the bridge node, which buffers the data from the sensors before sending it out on the Bluetooth link. By using a moderate buffer size of 12, we are able to keep the packet loss rate to < 2% on the phone. We also include a digital switch on the bridge to enable duty cycling of the Bluetooth radio.

In the following, we present detailed evaluation of AutoSense's power consumption profile as a function of sensor sampling rate, discuss antenna optimization for maximizing reliability of the wireless link when the sensor is placed close to the body, channel selection to minimize cross-technology interference from co-habiting wireless networks (Bluetooth, Wifi, Zigbee), and optimization of sensor sampling and wireless communication.

4.1 Obtaining Precise Energy Measurements

Modeling and estimating power consumption of wireless sensor nodes requires 1) precise current measurements in various modes of operation, and 2) extrapolation using a usage model to estimate the consumption profile of multiple protocols and sensing applications [28, 31]. Constructing a precise current consumption profile for a low-power, tightly integrated system such as AutoSense is a challenging task due to numerous software/hardware components affecting the current consumption across time. If digital switches are available across each hardware component, then one can enumerate all potential modes of operation and make measurements for alternatively powering each subcircuit using specialized hardware as in [9]. Here, we follow an alternative option where measurements are made on multiple channels at various points of the board simultaneously. The subcomponent current consumption is then calculated by differencing across time and channel.

In addition, conducting current measurements at μA resolution without loading the AutoSense circuit is not achievable with the standard method of inserting a shunt resistor and reading the voltage across it using an oscilloscope. To characterize the power consumption of the AutoSense sensor circuits and radio transceiver, we built a custom current measurement board using two Texas Instruments INA139 high

side current shunt monitor chips and 10 Ω SMT 1% current sense resistors. A dual channel configuration was made to allow for two simultaneous current measurements (*e.g.,* total sensor node current and radio current) with an output gain of 100. Our design provides higher reliability and quality control as compared to a simple sense resistor and probe measurement. The precision of the power measurement board is estimated to be +/- 10 μA.

4.2 Energy Profiling

Radio Transceiver. The MSP430 microcontroller unit (MCU) communicates with the nRF24AP2 through the SPI link to exchange the transmit and receive packets and control messages. Typically transceiver data sheets only report peak current power consumption for transmission and do not include current consumption during power cycling the radio and pulling the data in and out of the transceiver. With the newer transceiver designs, the RF power consumption during transmission is reduced dramatically, making the current consumption overhead for power-cycling and MCU serial communication non-negligible. We observe that although transmission of an 8 byte packet takes 150 μs, the setup time is significantly longer, and proper power consumption figures should include radio/MCU communication. Using the dual channel current measurement board, we conducted current measurements for the nRF24AP2 and nRF24AP2+MCU. Figure 4 shows the transmit power consumption trace for one packet. The peak power is approximately 15 mA. Therefore, the theoretically minimum transmit power consumption for a single packet is 15 mA*150 μs=2.25 μAs. The actual current consumption, however, includes the setup and release time of the radio which lasts 6.5ms and is given by the area under the current curve for nRF24AP2+MCU. It is 23.6 μAs (or, 70.8 μJ) per packet in our implementation; the per packet current consumption of just the nRF24AP2 transceiver is 18.9 μAsec (or, 56.7 μJ) per packet, which accounts for 80% of the power consumption. The energy efficiency of nRF24AP2 radio for our implementation is, therefore, 70.8 μJ/64 bits=1106 nJ/bit. (Four byte header that tags device and message type on each message is not counted as information bits). To compare this number to commercially available 802.15.4 transceivers, we conducted current measurements with the TelosB platform and found its efficiency to be 816 nJ/bit. While the overhead of small packet size of nRF24AP2 transceiver results in higher energy consumption per information bit, it provides TDMA protocol implementation with ultra low power standby current of 3 μA. Next, we combine this packet level measurement with sensor data rates to estimate the total lifetime of the AutoSense Mote for various data rates.

Sensor Boards. To characterize power consumption of the AutoSense sensors, we measured power consumption by enabling and disabling various components of the sensor system. We used the oscilloscope traces to determine the time duration of various tasks. The sensor chains have the following current consumption profiles — 210 μA for ECG+GSR and 1.48 mA for RIP. In addition, body and ambient temperature sensing consume 150 μA and the 3-axis accelerometer consumes 335 μA in steady state. The low sampling rate and

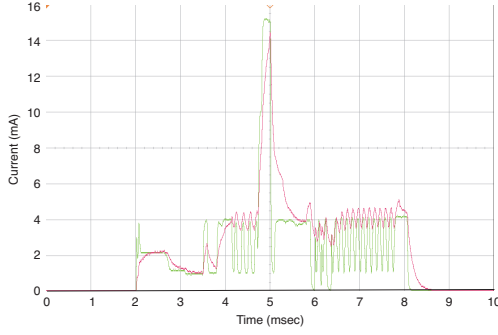**Figure 4. Current consumption per packet packet for Transceiver+MCU (red) and Transceiver Only (green) modes.**

Figure 5. Lifetime of AutoSense chestband mote as a function of sampling frequency

fast time constants of these sensors, however, enable power cycling on a per sample basis, rendering their contribution to power consumption to 60 μA. The above figures are for the analog sensor circuits only. Accurate lifetime calculations require consideration of MCU current consumption due to ADC sampling, conversion buffer access, and digital filtering. To simplify the power calculations, we consider two main power modes for the MCU — MCU executing background jobs waiting for sampling timer events μC(low), and MCU executing sampling and digital filtering μC(high). Table 2 summarizes the power consumption measurements.

Operation	Current Consumption
Sensors (I_1)	1.75 mA
Sensors+μC(Low) (I_2)	2.05 mA
Sensors+μC(High) (I_3)	3.82 mA
RadioTx (Average)(I_4)	3.63 mA

Table 2. Power Consumption for AutoSense

The radio setup and transmission last 6.5 *ms* for a 5 sample packet, whereas sampling and associated digital filtering takes, on average, 1 ms to execute. We can estimate the total current consumption as a function of sample rate f_s as:

$$I_{\text{total}} = 0.001 f_s I_3 + (1 - 0.001 f_s) I_2 + 0.0065 f_s / 5 I_4$$

On a 750 mAh battery, the total lifetime in days is given by $T_{\text{life}} = 750/(24 \times I_{\text{total}})$. Figure 5 shows the lifetime of AutoSense as a function of the overall sampling frequency. The circle denotes the operating point adopted in real-life deployments, which corresponds to 132 samples/sec (see Section 4.5.1), and results in an expected lifetime of 10.75 days.

4.3 Antenna Optimization for Body Sensors

AutoSense sensor motes use ceramic multilayer chip antennas from TDK with the reference tuning circuit from Nordic Semiconductor on our 4 layer board. Although the reference design provides nominal values for the tuning circuit, the antenna designed for free-space has to be optimized for placement close to the body. The human body affects
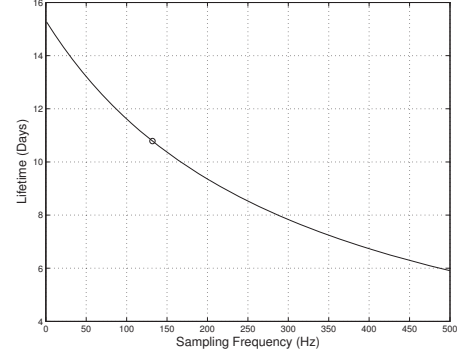
the antenna performance in two ways. First, the body's water content causes power loss in both receive and transmit modes. Second, the body acts as a ground plane, causing detuning of the antenna. The effect of the body on wireless propagation has been studied widely, and new antenna designs have been proposed for on body applications [3, 34]. Here, we evaluate the detuning effect and report the magnitude of performance degradation for commercial off-the-shelf chip antennas in close proximity to the body, variation of this degradation with distance from the body, and the effect of simple tuning circuits in recovering performance.

To ensure maximum efficiency in power transfer from the radio to the antenna, the input impedance of the radio should be matched to the output impedance of the transceiver set at 50 Ω. If the antenna impedance is mismatched, a portion of the incident wave to the antenna is reflected resulting in reduction of the transmitted power. The return loss (RL) measurements with a network analyzer provides the ratio of the power of the incident wave to the reflected wave for the antenna. A more practical measure of performance, the mismatch loss (ML), provides the reduction in the transmitted and/or received power due to mismatch of the antenna impedance. ML can be calculated from RL using $ML = 10\log(1 - 10^{RL/10})$. For optimizing antenna performance, the antenna measurements should be conducted at the same configuration (i.e., plastic casing, closeness to body etc.) of the intended deployment.

We performed return loss measurements for the ceramic chip antennas using the Agilent N5242A PNA-X network analyzer and a custom semi-rigid coax probe soldered to the board. The experimental setup is shown in Figure 6. The antenna return loss is measured when the PCB is placed at various distances from the body. The results are given in Figure 7. First, we observe that detuning is a function of the space between the PCB and the body. Therefore, optimization of the antenna should be conducted for the particular deployment configuration. Second, the result shows that the detuning becomes severe if no space exists between the PCB and the body. Therefore, we chose to include a small 25 mm spacing in our casing to temper the body effects.

We conducted a second set of measurements with the enclosure in place while the subject was wearing the sensors.

Based on these measurements, we implemented a matching circuit to bring the tuned frequency to 2.45 GHz. The results with and without the matching circuit are shown in Figure 8. We observe that without a proper tuning circuit, the return loss is -4.8dB, leading to 33.1% loss of transmission power. Since the loss will occur on both the transmit and receive ends this will lead to a -3.5dB power loss, resulting in a 35% decrease of the reliable communication range. In comparison, with input matching, the return loss is reduced to -20dB across the ISM band, with only -0.1dB power loss compared to ideal.
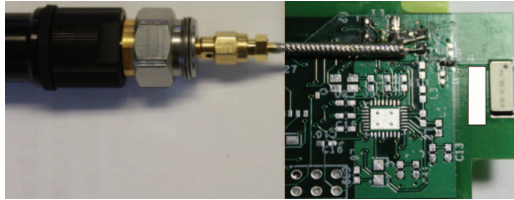

Figure 9. Antenna measurement of the final design with and without input matching. Return Loss (Left), Complex Reflection Coefficient in Smith Chart Form (Right)

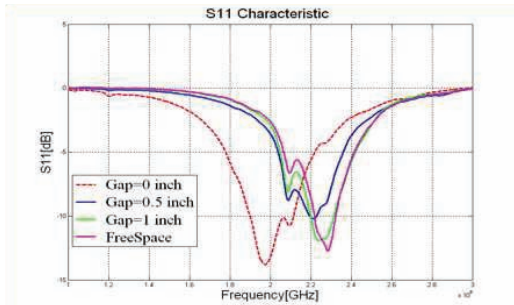**Figure 6.   Antenna measurement with custom co-ax probe**

Figure 7. Return Loss as a function of separation from Human Body
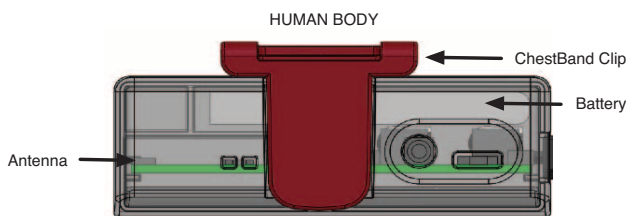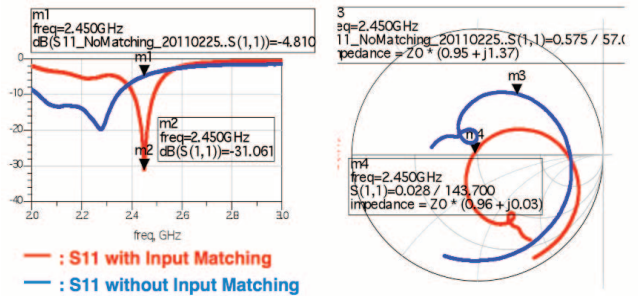

Figure 8. Custom enclosure design with antenna spacing

4.4   Using Empirical Study for Frequency Channel Selection

It has been observed that since 802.11 (WiFi), Bluetooth, and 802.15.4 (Zigbee) share the 2.4GHz ISM band, there is significant interference to 802.15.4 from WiFi, and therefore, the channel should be selected carefully to avoid high packet losses on the lower power radio due to interference from the higher power 802.11 radio [29]. This is the case with nRF24AP2 radio as well, since it shares the same 2.4GHz ISM band. In this section, we present empirical measurements of the packet delivery performance of the nRF24AP2 transceiver, which we use to select the appropriate frequency channel. The nRF24AP2 transceiver provides 125 frequency channels from 2400 MHz to 2524 MHz, separated by 1 MHz. We measured the interference from the eleven 802.11b channels to the 125 channels of our radio. The AutoSense chestband mote and the bridge mote were separated by 2 feet and a laptop was placed 6 feet from the two motes communicating with an access point, separated by a wall at 6 feet distance. For each 802.11b-nRF24AP2 channel pair, we recorded packet reception performance using 1,000 packets under two scenarios: (a) Background traffic to and from the access point encountered in a typical campus environment (b) Sustained data transfer to the laptop of a large file through FTP. The results are shown in Figure 10. We observe that under heavy traffic, the packet loss rate can be as high as 80%, if the channels overlap. For the channels that are outside the 802.11b band (2480-2524 MHz), the packet loss rate is low, at an average of 0.57%. These results guided us to use the frequency band, providing us with 45 individual usable channels. This is in addition to the TDMA diversity offered on each channel, each of which can support tens of coexisting radios. Consequently, TDMA diversity together with channel diversity provide sufficient scalability.

Since the loss rate is quite low on the 45 selected channels, we decided not to adopt the ACK handshake for retransmissions and simply mark the small percentage of missing data packets as non-valid data at the receiver end. This allows missing data to be handled appropriately by higher layers of inference algorithms.

4.5   Optimizing Sampling and Communication

As described earlier, the main driver of power consumption is the number of samples collected and passed over to the wireless link. AutoSense motes currently support two modes of sampling and processing, each optimized for the fixed rate link provided by the nRF24AP2 chipset — streaming mode and feature mode.

4.5.1   Streaming Mode

In the streaming mode, the sensor signals are first digitized at a sampling rate exceeding the analog bandwidth for each channel. We use the following sampling rates for the different biosignals — 128 Hz for ECG, 21.3 Hz for RIP, 10.7 Hz for GSR and Accelerometers, 2 Hz for body temper-
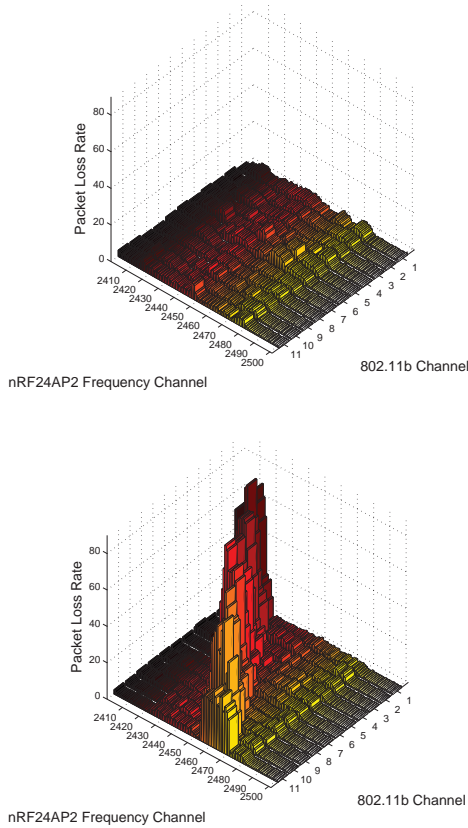
Figure 10. Packet Loss Rate for all channel pairs observed by the nRF24AP2 receiver through 802.11b traffic (a) Background and (b) Sustained data transfer

ature, and 1 Hz for ambient temperature and battery power sensors. The ECG is sampled at a high rate since location of R-peaks must be captured. Next, the ECG signal is fed to a digital low pass filter for the bandwidth to half with second order stable Infinite Impulse Response (IIR) filters implemented with fixed point arithmetic. The resulting ECG filter output is resampled at half the sampling rate, resulting in an output rate of 64 Hz. The aggregate output from all sensors is 132 samples/s.

The nRF24AP2 radio transceiver is configured to send data at a fixed rate using a TDMA scheme with a payload of 8 bytes/packet. Using 12 bits/sample and a 4 bit channel header, this provides 5 sensor samples per packet. We chose an operating point of 28 packets/sec to surpass the minimum required rate of 26.4 packets. This corresponds to an approximate output data rate of 1.8 Kbits/sec, which is less than 1/10th of the maximum allowed rate of 20kbits/s for the nRF24AP2. The nRF24AP2 expects buffers to be ready for each transmission slot at the given fixed rate, and data transmissions occur at the assigned timeslot irrespective of whether a packet has been handed to the radio transceiver. To maximize the efficiency of the TDMA protocol, we developed a fixed rate TDMA buffer manager. The TDMA buffer manager, whose basic structure is shown in Figure 11, employs two data buffers — regular sampled data buffers for

ECG, GSR, RIP. and accelerometer channels, and random sampled data buffers for body temperature, ambient temperature, battery power channels and system diagnostic data (buffer depths, sensor configurations, time synchronization). At the end of each packet transmission, the buffer manager fills the output buffer from the regular sampled data buffer if 5 consecutive samples are available from any of the sensor channels. Otherwise, the buffer manager fills the buffer from the random sampled data buffer. This buffer management is a simple scheme that provides all the available time slots with valid data, while allowing asynchronous independent operation of the sensor sampling and radio messages.
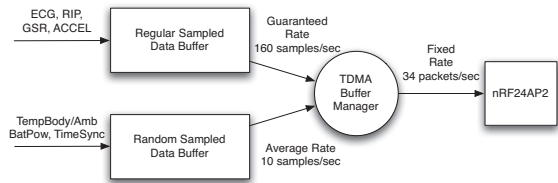

Figure 11. TDMA Buffer Manager

To preserve battery power, the TDMA scheme implemented by nRF24AP2 shuts down the radio between successive transmissions of data packets. Sampling, digital filtering, and resampling take 1.8ms per output sample, on average, at a 4 MHz clock frequency, occupying 58% of available CPU cycles for the AutoSense mote.

4.5.2 Feature Mode

Energy consumption can be further reduced if additional computation is performed locally on the mote. Providing the minimum rate of 64 Hz from ECG requires 12.8 packets/sec, making it the most significant source of power consumption due to frequent radio transmissions. Providing the preferred sampling rate for HRV at 512Hz will reduce the battery life drastically and preclude the possibility of continuous streaming of ECG signal with high sampling rate to a mobile computing platform for analysis. Instead, in the feature mode, we provide a distributed computation method for computing Heart Rate Variability (HRV) measures between the AutoSense Mote and a mobile computing platform. The mobile computing platform increases the beat detection resolution while reducing the required communication drastically. Figure 12 provides a flow diagram for the distributed HRV
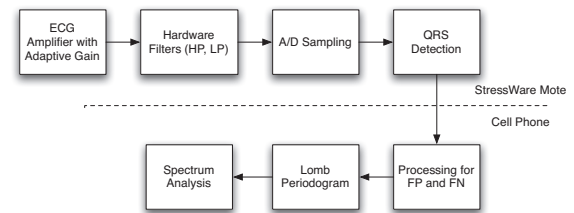

Figure 12. Distributed HRV computation

algorithm. The algorithm has three main components: 1) Local computation of potential beat locations with associated

confidence measures at the heart rate monitor, 2) Smoothing and interpolation using Gaussian Process Regression for labeling True and False Positives, and 3) Spectrum Calculation by Lomb-Periodogram on a mobile platform.

Potential R-wave locations are computed locally at the ECG Mote using a modified version of the QRS detection algorithm proposed by Hamilton-Tompkins [10]. The algorithm applies a series of filters to the data, followed by squaring and moving window integration. There are two adaptively running thresholds, based on signal and noise amplitude levels, for adapting to different ECG morphologies. The estimated position of beat events are periodically transmitted wirelessly to a mobile device. For a nominal heart beat frequency of 1 beat/sec, the beat locations require 13.2 packets per minute, assuming 10% false positive rate. This provides 58:1 reduction in communication bandwidth over the 12.8 packets/sec rate of the streaming mode. In the mobile device, an outlier removal algorithm based on peak-to-peak interval, normalized by mean and standard deviation over each minute, is used to reject too long or too short intervals.

4.6 Identifying Samples Lost in ANT Wireless Transmission

The short packet structure of 8 bytes supported by nRF24AP2 necessitates minimizing the overhead information sent as a header. The sensor node ID and sensor types are supported as part of the TDMA packet structure and does not count towards the payload of 8 bytes. However, sequence numbers are not included in the packet, which can be used to identify which samples were lost in the wireless transmission. Therefore, an explicit protocol needs to be agreed upon by the transmitter and receiver to be able to identify when data is lost in wireless transmission and determine the sensor type to which it corresponds to. Because of the fixed rate, the receiver is able to perceive that a packet was lost whenever no packet was received in the previously agreed upon timeslot. However, without any further knowledge, the receiver is not able to decipher the sensor channel that the missing packet corresponds to. To address this issue, we have chosen a fixed sampling/transmission schedule for the sensors that is based on a 4 bit sensor sampling counter, and we use a packet structure where five samples of 12 bits are augmented with this 4 bit counter to fill the 8 byte packets. Using the sensor sampling counter received before and after a sequence of missed packets, the receiver can determine how many of the missed packets were from the regularly sampled data buffer, and which sensor channels they correspond to. The bridge marks these samples as missing in the received sensor data buffers, so that missing data can be appropriately handled by higher level inference algorithms on a mobile device.

5 FieldStream: A Software Framework on Smart Phones

AutoSense sends sensor measurements to an Android mobile phone via a Bluetooth-to-ANT bridge. On the phone, the FieldStream software framework robustly collects sensor measurements, processes these measurements to produce inferences about the user (e.g., speaking from respiration, physical activity from accelerometers, and stress from ECG and respiration), and then shares these measurements and in-

ferences with subscribing external applications on the phone and logs them to a local database. Inferences are produced in real-time by the device (approximately 1-2 minutes after sensor measurements are collected, depending on the type of inference), allowing smart-phone applications to be responsive to changes in the body. For instance, self-report can be solicited from participants in a scientific study, if they are detected to be stressed.

5.1 Architecture

Figure 13 depicts how data flows through the FieldStream framework to produce inferences. First, the Android OS transports the raw byte stream from the bridge to the framework's **Network Layer** via the Android Bluetooth API. The Network Layer packetizes the raw byte stream and then demultiplexes the packets, identifying which sensor each packet corresponds to. Next, packets are passed to the **Windowing Layer** where they are added to an abstract sensor, a software abstraction of a sensor that buffers sensor data into windows. A window is a buffer of sensor data corresponding to a contiguous block of time, e.g., one minute. When a minute's worth of data is buffered in the window, the window is passed to the **Features Layer**.

The Features Layer calculates descriptors or features of the window using the **Feature Statistics Module** and **Virtual Sensors**. The feature statistics module computes basic statistics of a window, such as mean, variance, heart rate, and respiration rate. Virtual Sensors compute windows of intermediate features from other windows. For example, a virtual sensor could produce a window of R-peak locations from a window of ECG data, which are then further processed by the feature statistics module into heart rate. Once feature statistics are computed, they are passed on to the **Inferencing Layer**, where inferences are computed from the features.

Communication between the various layers is provided by a set of buses that follow the Observer design pattern [5]: a Mote Bus that passes packets from the Network Layer to the Windowing Layer; a Window Bus that passes windows from the Windowing Layer to the Features Layer; a Feature Bus that passes feature statistics from the Features Layer to the Inferencing Layer; and a Context Bus that passes context inferences to external applications. A logger listens on all the buses, and logs all sensor, feature, and context data for off-line post-processing and validation.

Several mobile phone applications have been built on top of FieldStream. These include an experience sampling program that collects self-reported ratings of stress from the user to validate stress inferences and an oscilloscope application for visualizing bodily indices (e.g., heart rate and respiration rate). Real-time health intervention applications, such as stress management, are under development.

5.2 Data Quality Monitoring

To meet the stringent data quality requirements of scientific studies, the system must provide the data quality controls of laboratory environments in the natural environment. Thus, FieldStream includes a data quality inferencing module that detects common situations that lead to lower quality data. When these situations are detected, the mobile phone informs the user and displays a set of actions he/she can take
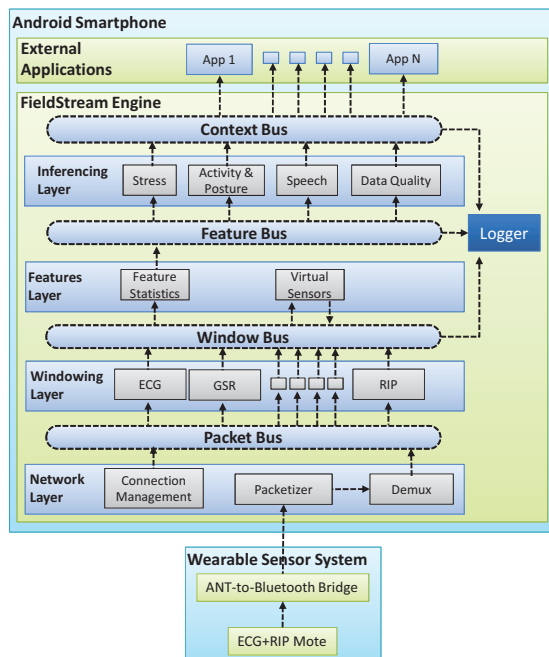
Figure 13. The FieldStream system, including the physical sensors, engine (Network, Windowing, Features, and Inferencing Layers), as well as the Mote, Window, Feature, and Context communication buses. Dotted arrows represent the flow of data through the system.

to correct them. For example, over the course of a day of wearing, an ECG electrode or a respiration band may gradually loosen from the user's body. This loosening results in a gradual degradation of ECG data quality over the course of day. Currently, FieldStream monitors four sensors for detachment or loosening — ECG and GSR electrodes, respiration band, and temperature probe attached to the chest. The details of this module are described in [22].

5.3 Handling Data Losses

Packets sent from the motes to the bridge or from the bridge to the phone could be lost in transmission. To ensure proper calculation of features and inferences, the system must be aware of these losses. SressWare and FieldStream handle lost data as follows. The bridge detects lost packets and inserts null packets in the data stream to replace them as described in more detail in Section 4.6. For losses incurred on the Bluetooth wireless channel, they are detected at the phone, using sequence numbers. The FieldStream network layer detects lost packets between the bridge and the phone and inserts null packets in the data stream. This effectively creates windows where some portion of the window corresponds to null packets. Features cannot be computed on these windows directly due to the null packets. Instead, virtual sensors serve as a filter. They decide if there is enough valid data in a window to compute accurate features of interest from that window. If there is not enough valid data in the

window (e.g., $< 66\%$), the window is discarded and no further processing occurs over it. If there is enough valid data, the null packets are removed from the window. If necessary, an additional processing stage may also occur to transform the valid data into a derived measurement (e.g., from ECG to RR intervals). The virtual sensor then sends the clean data onto the feature statistics module or onto another virtual sensor for further processing. The use of a virtual sensor as a filter on data losses means that feature computation and inferencing algorithms later in the pipeline do not need to individually implement custom strategies to deal with missing data.

6 Real-Life Deployment Experience

AutoSense was used by behavioral scientists in National Institutes of Health (NIH) sponsored scientific studies of stress, both in the lab and field. The goal of the study was to capture physiological response to stress in the lab and in the field so that reliable models for inferring stress from physiological measurements could be developed. 21 subjects were recruited from University of Minnesota, Duluth for this study. Each subject wore the AutoSense sensor suite and underwent a rigorous stress protocol that consisted of public speaking, mental arithmetic, and cold pressor test. The same participants then wore AutoSense during awake hours on two separate days in their natural environment. They provided frequent self-reports of stress both in the lab and in the field. Additional details of the study are provided in [23].

During the field study, physiological measurements from all sensors were wirelessly transmitted to the FieldStream framework running on an Android G1 smart phone. Over 30 features were computed from the physiological measurements to make four inferences — whether the subject is stressed, whether the subject is speaking (from respiration measurements) to help contextualize the inference of stress, changes in posture (from accelerometer) to again help contextualize the inference of stress, and intensity of physical activity. The latter was used to mark and filter out measurements overwhelmed by physical activity. In addition, the system automatically detected sensor detachments in real-time so that participants could re-attach sensors themselves.

6.1 Accomplishing User Study Goals

Overall, data collection statistics show AutoSense was able to reliably and robustly capture sensor data in natural environments. As described in [23], a total of 422 hours of data were collected from participants across the two days of the field study. The data captured by AutoSense enabled the development and evaluation of two models of stress that capture the physiological and psychological effects of stress, respectively [23]. Each model allows continuous prediction of stress from physiological measurements. The first model detects whether a minute of sensor data (respiration or ECG) is a physiological response to a stressor. The second model predicts whether a person perceives stress during a particular minute. As reported in [23], on lab data, the physiological classifier achieves 90% accuracy and the perceived stress model achieves a median correlation of 0.72 with self-reported rating of stress.

AutoSense and FieldStream together enabled modeling

of stress, a goal that has been sought after for decades. AutoSense enabled capture of high-quality ECG and respiration in natural environments, the key signals used to model stress in [23] and FieldStream provided a mechanism to capture self-reports in the natural environment and synchronize them with the signals captured by AutoSense.

6.2 Evaluation of Usability and Comfort

To evaluate the the usability and comfort of AutoSense for wearing in the field for long hours, we administered an exit survey at the end of the first and second field study days. Survey questions included whether the chestband was a nuisance, interfered with daily activities or social interactions, made the user feel self-conscious in public, caused physical discomfort, and was easy and enjoyable to use. Responses were provided on a 4 point scale (0=Strongly Disagree, 1=Disagree, 2=Agree, 3=Strongly Agree). No statistically significant differences were found between responses given after the first and second day. Thus, we average participant responses across both days in our analysis below.

Results show participants had positive reactions to the chestband. Participants felt that the chestband was easy ($Mean \pm Std.Dev = 2.06 \pm 0.3$) to use (ratings > 1.5 indicate agreement). They indicated it was not a nuisance (1.8 ± 0.6) and did not interfere significantly with daily activities (1.6 ± 0.6) or social interactions (2.0 ± 0.6). They were not self-conscious in public wearing the sensors (1.8 ± 0.7) and the chestband did not cause them significant physical discomfort (1.7 ± 0.7).

In extemporaneous comments to the study coordinators, some participants reported the RIP band and ECG electrodes caused some redness of the skin and itching after 12 hours of use. However, only one participant left the study after the first day of field study, implying this discomfort was not significant.

As the band must be worn about the upper chest, we expected some differences in the responses to these questions based on gender. Thus, we did a between-subjects comparison between male and female responses using two-tailed t-tests ($p < 0.05$ is statistically significant). Results show significant differences on four questions, whether the chestband was a nuisance ($p = 0.037$), interfered with daily activities ($p = 0.047$) and social interactions ($p = 0.01$), and made the participant feel self-conscious ($p = 0.008$).

Figure 14 depicts the differences between male and female responses on these four statements. While men and women both reported overall disagreement with these statements, the figure shows that, compared to women, men indicated the chestband was more of a nuisance, less socially acceptable, and interfered more with daily life. Based on comments provided by male participants, we speculate men were more concerned about these issues because, unlike women, men are not used to wearing undergarments on their chest. Furthermore, men may have been more self-conscious about the chestband in social situations, since the band would make them appear to have two protrusions on the chest which society does not expect men to have. These protrusions correspond to the location of the sensor motes.

The usability and comfort data has several implications for future designs of the system. In the future, the respira-

tion band should be padded to eliminate the itching. Longer wires connecting the single sensor mote to the electrodes and RIP band would also be useful, as it would allow moving thicker sensor motes away from the chest area. These changes would help reduce the concerns men expressed about the chestband.
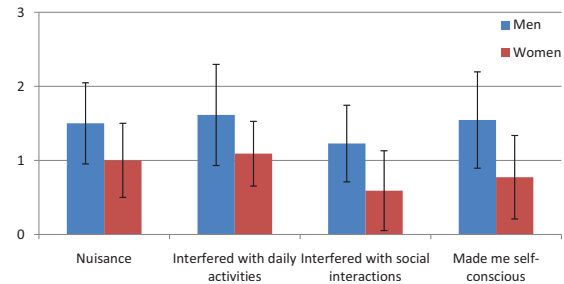

Figure 14. **Reported comfort and interference of the chestband in daily life across men and women (0=Strongly Disagree, 1=Disagree, 2=Agree, 3=Strongly Agree). Error bars depict 1 positive and 1 negative standard deviation away from the mean.**

6.3 Additional Ongoing Real-Life Usage of AutoSense and FieldStream

Due to its successful use in scientific studies of stress, there is a growing demand for use of AutoSense and Field-Stream in additional studies of stress. A 3-day field study has already been completed using AutoSense and FieldStream to study the effect of interruption on stress. Additional studies where AutoSense and FieldStream are worn by participants for multiple weeks in their natural environment are ongoing. Since April 2011, they are being used by 40 people over a one-week period to capture how stress influences smoking and alcohol consumption. Another 30 participants will begin using the sensor suite for four one-week periods in Fall 2011. In this study, the goal is to examine the relationship between stress, craving for illicit drugs (e.g., cocaine, heroin), and drug consumption. Over 50 sets of AutoSense sensor suites have been manufactured for use in these user studies.

7 Related Works

In this section, we discuss related works on physiological sensor suite, mobile phone framework, and those that have advanced modeling of human behaviors, privacy, or study designs by using the AutoSense and FieldStream platforms.

7.1 Physiological Sensor Suite

In the growing field of body sensor networks, a range of wearable platforms for monitoring physiological signals have been developed. Early platforms such as CodeBlue [16] and BSN [34] utilize 802.15.4 transceiver based platforms similar to Telos Mote to monitor ECG, temperature and SpO_2 vital signs. These systems enabled WSN researchers to experiment with vital signs monitoring applications with limited lifetime. More recent systems such as Berkeley Tricorder [20] that integrates ECG, EMG, Bioimpedance, and SpO_2 sensors, have improved signal quality and power consumption, but still have a lifetime of less than 24 hours.

For experimental work, several researchers use the SHIMMER platform [15]. It a wireless sensor platform for supporting long-term field studies that is fine-tuned for motion analysis. The design of the platform and the associated techniques for managing energy and radio bandwidth are matched to the motion and activity monitoring applications. While physiological sensors can be added to the platform, the resulting system would not cover all the modalities required for stress inferencing. Additionally, the power management techniques designed for accelerometer sensors would be suboptimal for the physiological sensor modalities.

Similarly, commercially available wearable sensors for collecting physiological measurements from the field have one or more of the following shortcomings. They have only a few sensors, are cumbersome to wear on a daily basis without causing social embarrassment, or have a short lifetime. For example, LifeShirt from Vivometrics is a vest-like device that can monitor ECG, respiration, skin temperature, and physical activity. However, this wired system is bulky, expensive, and uses proprietary wireless technology not compatible with mobile phones. An increasingly popular wireless health monitor called BioHarness BT from Zephyr Technologies provides several measures, such as ECG, respiration, skin conductance, temperature, and activity, which are transmitted to a mobile phone using Bluetooth. The main drawback of BioHarness is its lifetime of only 24 hours.

In summary, most existing wearable sensor platforms that can be used for continuous monitoring of physiological measurements needed for robust stress assessment in the natural environment have a lifetime of at most 24 hours. AutoSense, on the other hand, is able to provide more than 10 days lifetime while continuously sampling and transmitting all six sensors it hosts. Additionally, AutoSense is able to provide virtually loss free and timely wireless transmission of sensor measurements that is tolerant to proximity to human body, tolerant to interference from other co-habiting wireless networks (e.g., Wi-Fi and Zigbee), and tolerant to crowding scenarios.

7.2 Mobile Phone Platforms

In comparison to existing inferencing systems for mobile phones, FieldStream is most similar to the MyExperience system. MyExperience [4] collects objective data about study participants on a mobile phone and triggers collection of subjective data from participants based on simple context. The MyExperience architecture is built on 3 core components, sensors, triggers, and actions. Triggers are sets of conditional logic on multi-modal sensor data. When a trigger is true, its corresponding action is taken (e.g., prompt for self-report). FieldStream shares other characteristics with previous mobile phone context inferencing systems. Two examples include the use of a dynamic activation manager that only enables sensors and features that are needed by active inferencing modules, and reducing resource usage (CPU, battery) by doing a computation once and sharing the result with all modules that need it [11, 32].

The JigSaw framework is designed to optimize sensing pipelines for sensors commonly embedded in smartphones (accelerometer, microphone, and GPS) [17]. JigSaw's accelerometer pipeline produces robust outputs under a variety of positions and orientations. In addition, JigSaw reduces energy consumption by deactivating or throttling down sensing pipeline when behavioral inferences indicate they are unlikely to provide new or high quality data.

FieldStream differs from the above systems in five ways. First, FieldStream is capable of more sophisticated inferencing than has been demonstrated in previous mobile-phone-based systems. It uses sophisticated signal processing to compute features and can infer if a person is stressed [23] or speaking [24] from those features. Second, FieldStream uses hierarchical buses to share data and computation among system entities. Third, FieldStream is capable of collecting and processing data from both external wireless sensors and sensors embedded in the smartphone. Fourth, FieldStream detects sensor detachments and provides instructions to the user on how to correct the problem in the field. Fifth, to our knowledge, FieldStream is the only mobile sensing framework that has been evaluated in the context of real-life scientific field studies for several days [23, 25].

7.3 Usage of AutoSense and FieldStream Platforms

In this paper, we present innovations in the development of the AutoSense hardware platform and FieldStream mobile phone software platform that was used to collect reliable data from natural environment for various user studies, which enabled development of new models of stress [23] and new models of conversation [24]. It was also used in another user study that led to the discovery of new privacy issues in the usage of mHealth systems [25] and exploration of appropriate microincentive structures for participant compensation in mobile health user studies [19]. Specifically, the above cited works are investigations in modeling, privacy, and study designs that use the data collected and annotated by the Autosense and FieldStream systems. These are only the first milestones in inferring human states and behaviors. Other researchers are encouraged to use Autosense to conduct new field studies and/or analyze the data collected by others. In future, AutoSense and FieldStream platforms will be used to develop models for inferring additional human behaviors or health conditions of interest such as smoking, drinking, craving, etc. and to study the efficacy of new mHealth interventions. We envision the AutoSense and FieldStream platforms to become a comprehensive mobile health platform that can be used to monitor various physical, mental, and behavioral health issues, and to administer timely interventions in the natural environment of individuals.

8 Conclusion and Future Work

AutoSense provides a comprehensive suite of ultra-low power sensors that can be worn unobtrusively in the natural environment of subjects to enable collection of physiological measurements associated with stress response. Wireless transmission to a mobile phone in real-time, makes it possible to realize several goals such as monitoring of physiological responses to real-life stressors, objective and continuous estimation of stress, triggering of self-reports close to the occurrence of stress events, delivering interventions on mobile devices close to the occurrence of stress, among others. Additional sensors are being integrated in another sens-

ing unit to assess addictive behavior such as alcohol. Taken together, AutoSense will provide measurement of stress and various behaviors that may be related to stress such as drinking, smoking, physical activity, movement patterns, conversations, etc. all on a single comprehensive platform, making it a suitable platform for study of physical, behavioral, and mental health in the natural environment. In future, scientific studies can yield effective prevention and intervention applications, which can be delivered on the mobile phone in the mobile environment, realizing the vision of mobile health.

9 Additional Authors

Somnath Mitra (University of Memphis, email: smitra3@memphis.edu), Taewoo Kwon, (The Ohio State University, email: kwonta@cse.ohio-state.edu), and Jae Woong Jeong (The Ohio State University, email: jeongj@ece.osu.edu)

10 References

[1] ANT technology homepage. http://www.thisisant.com.

[2] D. Alexander, C. Trengove, P. Johnston, T. Cooper, J. August, and E. Gordon. Separating Individual Skin Sonductance Responses in A Short Interstimulus-Interval Paradigm. *Journal of neuroscience methods*, 2005.

[3] A. Alomainy, Y. Hao, and D. Davenport. Parametric study of wearable antennas with varying distances from the body and different on-body positions. In *2007 IET Seminar on ntennas and Propagation for Body-Centric Wireless Communications*, pages 84–89, April 2007.

[4] J. Froehlich, M. Chen, S. Consolvo, B. Harrison, and J. Landay. MyExperience: a system for in situ tracing and capturing of user feedback on mobile phones. In *ACM MobiSys*, page 70, 2007.

[5] E. Gamma, R. Helm, R. Johnson, and J. M. Vlissides. *Design Patterns: Elements of Reusable Object-Oriented Software*. Addison-Wesley Professional, 1994.

[6] G. Giorgetti, G. Manes, J. Lewis, S. Mastroianni, and S. Gupta. The personal sensor network: A user-centric monitoring solution. In *BodyNets*, 2007.

[7] P. Grossman, F. Wilhelm, and M. Brutsche. Accuracy of Ventilatory measurement employing ambulatory inductive plethysmography during taskS of everyday life. *Biological Psychology*, 2010.

[8] J. Healey and R. Picard. Detecting stress during real-world driving tasks using physiological sensors. *IEEE Transactions on intelligent transportation systems*, 6(2):156–166, 2005.

[9] X. Jiang, P. Dutta, D. Culler, and I. Stoica. Micro power meter for energy monitoring of wireless sensor networks at scale. In *ACM IPSN*, pages 186–195, 2007.

[10] J.Pan and W. Tompkins. A real-time ors detection algorithm. *IEEE Trans. on Biomed Eng*, (3):220–236, 1985.

[11] S. Kang and et. al. SeeMon: scalable and energy-efficient context monitoring framework for sensor-rich mobile environments. In *ACM MobiSys*, 2008.

[12] S. Kreibig. Autonomic Nervous System Activity in Emotion: A Review. *Biological Psychology*, 2010.

[13] S. Kreibig, F. Wilhelm, W. Roth, and J. Gross. Cardiovascular, electrodermal, and respiratory response patterns to fear-and sadness-inducing films. *Psychophysiology*, 44(5):787–806, 2007.

[14] M. Lee, G. Yang, H. Lee, and S. Bang. Development stress monitoring system based on personal digital assistant. In *Proc. of 26th Annual International Conference on Engineering in Medicine and Biology Society*, 2004.

[15] K. Lorincz, B. Chen, G. Challen, A. Chowdhury, S. Patel, P. Bonato, and M. Welsh. Mercury: A Wearable Sensor Net-

[16] K. Lorincz, D. Malan, T. Fulford-Jones, A. Nawoj, A. Clavel, V. Shnayder, G. Mainland, M. Welsh, and S. Moulton. Sensor networks for emergency response: Challenges and opportunities. *IEEE pervasive Computing*, pages 16–23, 2004.

[17] H. Lu and et al. The Jigsaw Continuous Sensing Engine for Mobile Phone Applications. In *ACM SenSys*, 2010.

[18] D. McFarland. Respiratory markers of conversational interaction. *Journal of Speech, Language, and Hearing Research*, 44(1):128–143, 2001.

[19] M. Mustang, A. Raij, D. Ganesan, S. Kumar, and S. Shiffman. Exploring Micro-Incentive Strategies for Participant Compensation in High Burden Studies. In *ACM CHI*, 2011.

[20] R. Naima and J. Canny. The berkeley tricorder: Ambulatory health monitoring. In *IEEE BSN*, pages 53–58, 2009.

[21] N. A. Nicolson. *Handbook of Physiological Research Methods in Health Psychology*, chapter Measurement of Cortisol. SAGE Publications, 2007.

[22] K. Plarre, A. Raij, S. Guha, and S. Kumar. Automated Detection of Sensor Detachments for Physiological Sensors in the Wild. In *ACM Wireless Health*, 2010.

[23] K. Plarre, A. Raij, M. Hossain, A. Ali, M. Nakajima, M. al'Absi, E. Ertin, T. Kamarck, S. Kumar, M. Scott, D. Siewiorek, A. Smailagic, and L. Wittmers. Continuous Inference of Psychological Stress from Sensory Measurements Collected in the Natural Environment. In *ACM/IEEE IPSN*, 2011.

[24] M. M. Rahman, A. A. Ali, K. Plarre, A. Raij, M. alAbsi, E. Ertin, and S. Kumar. mConverse: Inferring Conversation Episodes from Respiratory Measurements Collected in the Field. In *ACM Wireless Health*, 2011.

[25] A. Raij, A. Ghosh, S. Kumar, and M. Srivastava. Privacy Risks Emerging from the Adoption of Inoccuous Wearable Sensors in the Mobile Environment. In *ACM CHI*, 2011.

[26] P. Rainville, A. Bechara, N. Naqvi, and A. Damasio. Basic emotions are associated with distinct patterns of cardiorespiratory activity. *International journal of psychophysiology*, 61(1):5–18, 2006.

[27] R. Sapolsky. *Why zebras don't get ulcers*. Owl Books, 2004.

[28] V. Shnayder, M. Hempstead, B. Chen, G. Allen, and M. Welsh. Simulating the power consumption of large-scale sensor network applications. In *ACM SenSys*, pages 188–200, 2004.

[29] K. Srinivasan, P. Dutta, A. Tavakoli, and P. Levis. An empirical study of low-power wireless. *ACM Transactions on Sensor Networks (TOSN)*, 6(2):1–49, 2010.

[30] J. F. Thayer, A. L. Hansen, and B. H. Johnsen. *Handbook of Physiological Research Methods in Health Psychology*, chapter Noninvasive Assessment of Autonomic Influences on the Heart. SAGE Publications, 2007.

[31] Q. Wang, M. Hempstead, and W. Yang. A realistic power consumption model for wireless sensor network devices. In *IEEE SECON*, volume 1, pages 286–295, 2006.

[32] Y. Wang, J. Lin, M. Annavaram, Q. Jacobson, J. Hong, B. Krishnamachari, and N. Sadeh. A framework of energy efficient mobile sensing for automatic user state recognition. In *ACM MobiSys*, 2009.

[33] F. Wilhelm and P. Grossman. Emotions beyond the laboratory: Theoretical fundaments, study design, and analytic strategies for advanced ambulatory assessment. *Biological Psychology*, 2010.

[34] G. Yang. *Body sensor networks*. Springer-Verlag New York Inc, 2006.